where $v(\vec{q})$ is the Fourier transform of the Coulomb potential. In this fashion one may also account for plasma polarizability in the case of more complex contributions to $\bar{\sigma}^{\pm}(\vec{k})$.

Since the nonequilibrium expansion is identical to that of the equilibrium expansion, the effect of polarizability on $\sigma^{<}$ is easily determined.

*Work performed under the auspices of the U. S. Atomic Energy Commission.

[1]B. Bezzerides, J. Quant. Spectry. Radiative Transfer 7, 353 (1967).
[2]G. P. Reck, Hisao Takebe, and C. Alden Mead, Phys. Rev. 137, A683 (1964).
[3]U. Fano, Phys. Rev. 131, 259 (1963).
[4]M. Baranger, Phys. Rev. 112, 855 (1958).
[5]H. Margenau and M. Lewis, Rev. Mod. Phys. 31, 569 (1959).
[6]J. S. Langer, Phys. Rev. 127, 5 (1962).
[7]D. F. DuBois, V. Gilinsky, and M. G. Kivelson, Phys. Rev. 129, 2376 (1963).
[8]B. Bezzerides and D. F. DuBois, Phys. Rev. 168, 233 (1968).
[9]G. Birnbaum, Phys. Rev. 150, 101 (1966).
[10]B. Bezzerides, Phys. Rev. 159, 3 (1967).
[11]R. G. Breene, The Shift and Shape of Spectral Lines (Pergamon Press, New York, 1961).
[12]E. W. Smith and C. F. Hooper, Jr., Phys. Rev. 157, 126 (1967).
[13]R. H. Dicke, Phys. Rev. 89, 472 (1953).
[14]C. F. Hooper, Jr., Phys. Rev. 149, 77 (1966).
[15]B. Mozer and M. Baranger, Phys. Rev. 118, 626 (1960).
[16]G. Baym and L. P. Kadanoff, Quantum Statistical Mechanics (W. A. Benjamin Inc., New York, 1962).
[17]D. W. Ross, Ann. Phys. (N. Y.) 36, 458 (1966).
[18]A. A. Abrikosov, L. P. Gonkov, and I. A. Dzyaloshinski, Methods of Quantum Field Theory in Statistical Physics (Prentice-Hill, Englewood Cliffs, New Jersey, 1963).
[19]M. Baranger, Atomic and Molecular Processes edited by D. R. Bates (Academic Press, Inc., New York 1962), p. 530.
[20]M. Baranger and B. Mozer, Phys. Rev. 123, 25 (1961).
[21]W. Cooper, private communication (to be published).
[22]R. E. Cutkosky, J. Math. Phys. 1, 429 (1960).

PHYSICAL REVIEW VOLUME 181, NUMBER 1 5 MAY 1969

Liquid-Solid Phase Transition in He^3-He^4 Mixtures*

P. M. Tedrow[†‡] and D. M. Lee
Laboratory of Atomic and Solid State Physics, Cornell University, Ithaca, New York 14850
(Received 22 July 1968)

Measurements on the liquid-solid phase transition of He^3-He^4 mixtures have been performed by means of a strain-gauge technique. It was found that the freezing curves of mixtures with initial concentrations of greater than 5% He^3 merged into a common curve with negative slope in the P-T plane. This curve is interpreted to be a three-phase equilibrium line or univariant involving the coexistence of bcc solid helium and the two phase-separated liquids, one rich in He^3 and the other rich in He^4. A number of other univariant lines involving these and other phases of helium have also been observed. Univariants intersect at quadruple points which are defined as points where four phases coexist. A quadruple point has been observed in these experiments involving coexistence of bcc solid helium, hcp solid helium, and the two phase-separated liquids at a temperature $T = 0.37$°K and a pressure $P = 26$ atm. The data is discussed in terms of a three-dimensional phase diagram which is consistent with the Gibbs phase rule and with the results obtained by other investigators.

I. INTRODUCTION

A number of interesting phenomena have been observed in liquid and solid He^3-He^4 mixtures. Phase separation below about 0.85°K in the liquid mixtures was first discovered by Walters and Fairbank.[1] The maximum temperature at which phase separation occurs was found to be lowered

as the pressure on the sample increased.[2] It has recently been observed that He^3 remains soluble in He^4 in concentrations less than about 6.3% down to absolute zero.[3,4] Phase separation was discovered in solid mixtures of He^3 and He^4 below 0.38°K by Edwards, McWilliams, and Daunt.[5] A crystallographic phase transition between a body-centered cubic (bcc) and a hexagonal close-packed (hcp) solid phase has been studied in He^3-He^4 mixtures by Vignos and Fairbank.[6] Both pure He^3 and pure He^4 have regions of negative slope in their freezing curves.[7-9] Similar behavior has been noted in He^3-He^4 mixtures in this laboratory[10] and at Leiden.[11]

In this paper, measurements on the liquid-solid phase transition of He^3-He^4 mixtures, primarily by strain-gauge techniques, are described. The measurements were carried out at temperatures below 1.5°K, pressures from 20 to 40 atm and concentrations from 0 to 100% He^3. A phase diagram is deduced which is consistent with the Gibbs phase rule, the results of these experiments, and the results discussed in Ref. 1-9. Preliminary results of the investigations described in this paper have been published previously.[10,12,13] The results of parallel investigations at other laboratories are compared with the present results.

II. APPARATUS

Two different experimental chambers were employed to obtain the data presented here. The first, shown in Fig. 1, provided the bulk of the data above 0.4°K while the second, shown in Fig. 2, was used at temperatures down to about 0.15°K. Both designs made use of strain gauges in order to provide pressure measurements when the fill line was blocked with solid, isolating the chamber from the external pressure gauge. This experimental technique is similar to that used by Baum *et al.*[7]

The first apparatus consisted of a hollow copper cylinder containing a nuclear magnetic resonance (NMR) coil. A 1.27-cm-diameter brass sleeve with a 0.015-cm wall fitted over this cylinder and was soft soldered at both ends. An annular region 0.008-cm wide between the brass sleeve and copper cylinder contained the sample. Two 0.079-cm holes connected the annular region with the cavity containing the NMR coil. The sample entered the chamber by means of a 0.015-cm-i.d. Cu-Ni capillary. The strain gauge, a Baldwin SR-4 120-Ω transducer,[14] was glued to the center of the brass sleeve. A second gauge glued to the copper block served as a dummy for temperature compensation. The difference in resistance of the two gauges was measured using a modified Blake-Chase-Maxwell 32-Hz bridge.[15]

A Speer 470-Ω, $\frac{1}{2}$ W resistor[16] was used to measure the temperature. This resistor was cal-

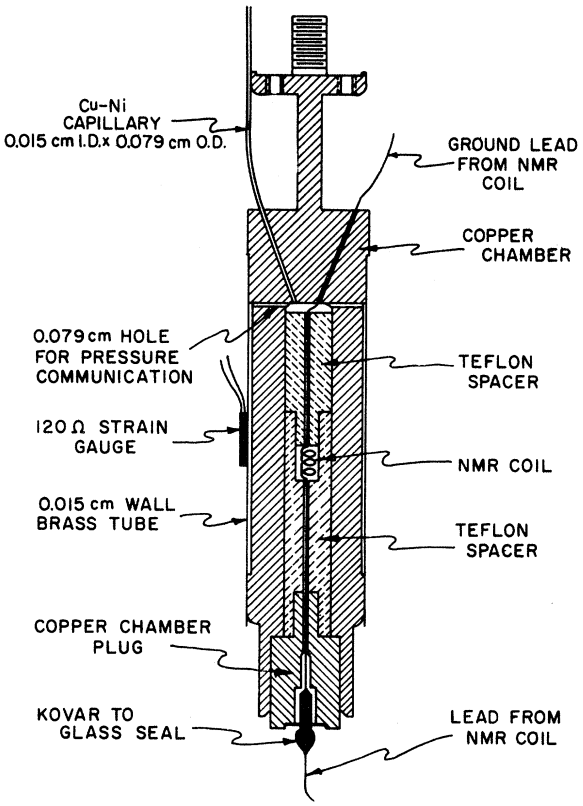

FIG. 1. The first apparatus.

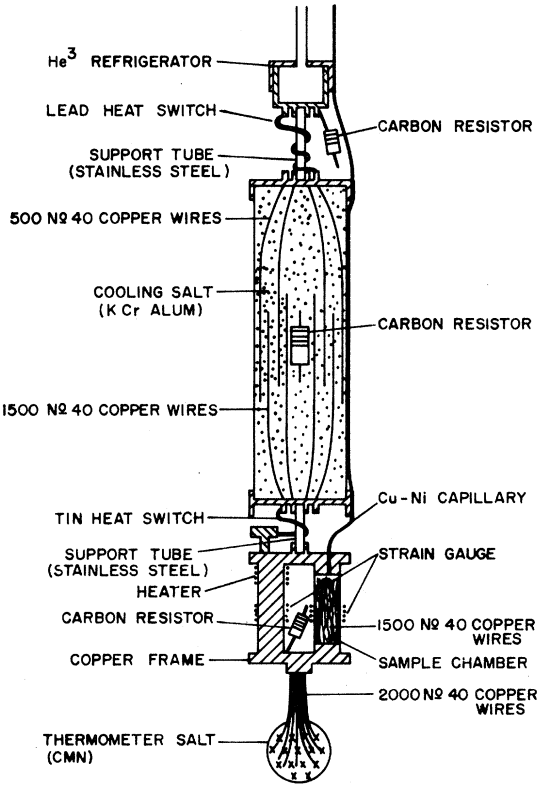

FIG. 2. The second apparatus.

ibrated using the vapor pressure of the He^4 bath, the vapor pressure of He^3, and the nuclear susceptibility of solid He^3 near the melting curve. The resistance was measured using a 25-Hz bridge.

The He^4 bath was pumped to 1°K, and the He^3 refrigerator cooled the apparatus to 0.37°K. To provide isolation from the He^4 bath, the apparatus was enclosed in a brass exchange gas can which was soldered in place using Wood's metal. The electrical leads emerged from the exchange gas can through Kovar-glass seals. We used cw NMR measurements, similar to those described earlier,[17] to determine when solid was present in the chamber. The solid possesses a much shorter longitudinal relaxation time T_1 than the liquid, making the solid resonance more difficult to saturate. The presence of a resonance signal which was difficult to saturate indicated that solid was present in the chamber.

Unfortunately, the magnetic field necessary for the NMR measurement adversely affected the strain gauges, making it impossible to use the two techniques simultaneously. It was necessary to thermally cycle the gauges in order to obtain meaningful data after they had been exposed to the magnetic field.

To obtain data at lower temperatures, the second apparatus was constructed. Figure 2 shows the part of the cryostat which was cooled below 1°K and which was contained in an exchange gas can that was immersed in the He^4 bath. This apparatus made use of adiabatic demagnetization of the paramagnetic salt, chromium potassium alum (KCr Alum) to obtain temperatures below 0.35°K. The apparatus was also designed for specific-heat measurements of the mixtures as a function of temperature and pressure.

The chamber itself consisted simply of a 2.5-cm-long, 0.64-cm-diameter, 0.015-cm-wall stainless-steel tube into whose ends were soft-soldered copper end pieces. As shown in Fig. 2, a copper rod was soldered between the end pieces to complete the copper support frame. About 1500 bare No. 40 AWG copper wires, hard soldered to the lower copper end piece, filled nearly half the volume of the chamber and furnished thermal contact within the stainless-steel tube. An 0.028-cm-i.d. Cu-Ni capillary entered the chamber through the top end piece to admit the sample.

The strain gauge was fabricated from about 120 cm of No. 40 AWG Advance[18] wire, heavy Formvar insulated, wrapped non inductively around the center of the stainless-steel tube, and secured with household cement.[19] A similar gauge was wound on the copper rod for temperature compensation. It was possible to detect pressure changes of 0.04 atm with these strain gauges.

Temperature measurements were made using an $8\frac{1}{2}$-Hz ac mutual-inductance bridge to measure the paramagnetic susceptibility of a cerium magnesium nitrate (CMN) pill thermally attached to the chamber. Primary and secondary coils were situated outside the exchange gas can in the He^4 bath. The CMN pill contained about 10 g of the powered salt and was held together by Castolite,[20] a thermosetting plastic. Thermal contact to the sample was provided by 2000 insulated No. 40 AWG copper wires which were hard soldered to the lower end piece of the sample chamber. A Speer 470-Ω, $\frac{1}{2}$-W carbon resistor was also soldered to the lower end piece for use as a secondary thermometer. A heater, made from 230 cm of No. 40 AWG Advance wire and having a resistance of 210 Ω was wound on the copper frame and secured with varnish.

All the electrical leads initially were No. 30 AWG Advance wire. Later, the strain-gauge leads were changed to No. 30 AWG niobium wire in an effort to avoid magnetic problems. The niobium leads were spot welded to small pieces of nickel sheet, which were then soldered to No. 36 AWG copper wires which in turn were soldered to the strain gauges.

The experimental chamber was suspended from the cooling salt pill by means of a 0.32-cm-diameter, 0.009-cm-wall stainless-steel tube. The refrigerator salt pill was 10-cm long and 2.5 cm in diameter and contained about 60 g of potassium chrome alum salt. About 1500 No. 40 AWG copper wires distributed through the salt were soldered to a copper plate at the bottom of the salt to provide thermal contact with the sample chamber, while about 500 separate No. 40 AWG copper wires extended upward through the salt to the copper top plate to provide contact through a lead heat switch to the He^3 refrigerator. The wires and salt were again bonded together with Castolite. The heat switch was a strip of 99.999%-pure lead, 3.8-cm long, 0.6-cm wide, and 0.025-cm thick, fastened at each end with Wood's metal. A similar heat switch of 99.999% pure tin was used to connect the salt pill with the sample chamber. This switch was later replaced by a copper strap when specific-heat measurements were completed. The salt pill was suspended from the He^3 refrigerator by a 0.32-cm diameter, 0.009-cm wall stainless-steel tube 2.5-cm in length.

A solenoid rated at 15 kG with a persistent current switch supplied the field for demagnetization. The magnet was suspended by a stainless-steel tube which extended through a sliding "O" ring seal at the top of the cryostat so that the magnet could be raised to remove it from the region of the strain gauges.

Difficulties were caused by magnetic field effects giving rise to poor reproducibility in the strain gauges. In order to remove these magnetic field effects as much as possible, the Advance leads from the strain gauges were replaced with niobium, and a superconducting lead shield was

placed above the chamber to protect it from the magnetic field. With this configuration, the strain gauges in the second apparatus functioned reproducibly at temperatures below about 0.5°K. Thus it was possible to use the overlap with data taken with the first apparatus to obtain reliable measurements over the entire temperature range even though the strain gauges were still unreliable above 0.5°K.

III. EXPERIMENTAL PROCEDURE

To make the samples, pure He^3 gas and pure He^4 gas were mixed in a glass manifold incorporating two $\frac{1}{2}$-liter Toepler pumps. The concentrations were determined by measuring the pressure of a fixed volume of each constituent. The ratio of the pressure of He^3 so obtained to the total of the He^3 and He^4 pressures was taken to be the concentration.

With the first apparatus, after the helium bath had been pumped down to the desired temperature, the sample was admitted and the pressurization was carried out in the following way: A known gas volume of a given He^3 concentration was condensed into a 1.5-cm^3 copper chamber which was immersed in a small auxiliary Dewar containing liquid He^4 at 1.3°K. A capillary connected the copper chamber with the sample chamber in the main cryostat and with an external Bourdon pressure gauge.[21] The copper chamber, the sample chamber, and the Bourdon gauge were then isolated from the glass gas-handling system by means of a high-pressure ball valve. The copper chamber was then removed from the auxiliary Dewar producing pressures up to 40 atm. The pressurization was normally carried out when the temperature of the sample chamber was below 1.3°K. The temperature was chosen so that when the final pressure was achieved, the sample was still entirely liquid. With pressurization completed, the helium bath was pumped to about 1°K. After the He^4 exchange gas was removed, the He^3 refrigerator was started and the sample was cooled at a speed appropriate for taking data and for maintaining equilibrium. The strain gauges were calibrated against the external pressure gauge using sample pressures below those needed to form solid. Separate runs were made to determine the small temperature dependence of the strain gauges in order to make the necessary corrections.

The procedure with the second apparatus was only slightly more complicated. As the outer helium bath was pumped down, the susceptibility of the CMN salt was calibrated against the vapor pressure of He^4. The procedure for pressurizing the sample was identical to the procedure with the first apparatus. When the bath reached its lowest temperature, about 1.3°K, the magnet was positioned and turned on. With the heat of magnetization of the KCr alum salt removed, the exchange gas was pumped out and the He^3 refrigerator started. When the sample chamber and the salt pill had cooled to 0.7°K, the magnet was turned off in about 3 min. When the tin heat switch was in use, the field was at first reduced to a level just above the critical field of tin and was held at this value until the chamber reached its lowest temperature. The field was then reduced to zero, allowing the tin to become superconducting and thermally isolating the chamber for specific-heat measurements. Later, with a copper strap replacing the tin, the field could be reduced to zero without stopping. The magnet was then raised to remove it from the vicinity of the strain gauges and the CMN.

The specific-heat measurements were made with the help of an electric timer which automatically turned off the heater power after a preset time interval. A measured amount of heat was added using the heater and the resulting change in temperature was noted. The amount of heat added was determined by measuring the voltage across and the current through the heater.

The freezing curve of a mixture is the locus of points in the P-T plane where solidification begins to take place. The melting curve is the locus of points where melting begins. These two curves coincide for pure substances, but in general do not coincide for mixtures.

The freezing curves were obtained in several different ways. In method (1) the NMR signal could be used to detect the first formation of solid as the sample was cooled at constant pressure. Since the solid has a shorter spin-lattice relaxation time than the liquid, the onset of solidification was easy to observe. A repetition of this procedure at different pressures made it possible to map out the freezing curve. This method was useful only for the positive-sloped region of the freezing curve where the capillary remained open and pressure communication with the external pressure gauge was possible.

In method (2) the strain-gauge reading and the temperature were monitored continuously and plotted on a P-T diagram. This method gave fairly accurate results for the negative-sloped region of all the mixtures because in this region, the curve did not depend on concentration. A difficulty arises in the positive-sloped region owing to the difference between the liquidus and solidus. Variations in starting pressure and sample volume could change the path of the experiment through the two-phase region of the PTX space. For the 24.2% and 38.4% mixtures, however, the difference between liquidus and solidus is not too great. The curves measured for these mixtures are nearly independent of the starting pressure. At higher He^3 concentrations there is a considerable spread

between liquidus and solidus. The difficulty is illustrated in Fig. 3 which shows a series of runs with different initial pressures for an 82.3% mixture where a substantial difference exists between the locations of liquidus and solidus. Different starting pressures lead to a variety of different curves.

Method (3) is similar to method (1) except the strain gauges are used to detect the formation of solid. The sample is cooled at constant external pressure, starting at a temperature higher than that at which solidification takes place. When solidification begins, the fill line blocks and the pressure in the chamber drops as further solid forms. Thus the strain-gauge readings show an abrupt change in slope (kink) as a function of temperature as shown in Fig. 3. The locus of these kinks in the P-T plane is the freezing curve for the mixture.

A similar method can be used to measure melting curves. With the sample at a high pressure, the He^3 refrigerator was employed to cool the apparatus. Pressure versus temperature measurements were taken. At sufficiently low temperatures, the P versus T curve would become horizontal, showing that the chamber was full of solid. The point at which this kink occurred yielded a point on the melting curve (solidus) for the mixture.

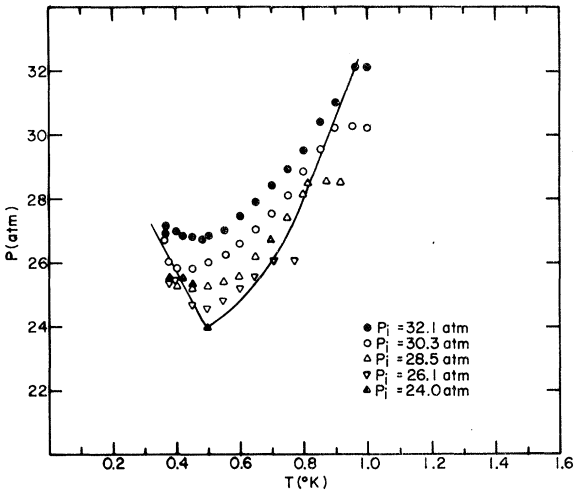

FIG. 3. Strain-gauge measurements on an 82.3% mixture of He^3 in He^4 for several starting pressures. The solid line is the freezing curve for this mixture. Because of the large separation of liquidus and solidus for this mixture, the data depends strongly on starting pressure P_i.

IV. RESULTS AND DISCUSSION

A. Freezing-Curve Measurements Above 0.4°K

Figure 4 shows smoothed freezing-curve measurements for pure He^4 and mixtures with He^3 concentrations of 4.69%, 18.8%, 24.2%, and 38.4% obtained with the first apparatus. These curves are averages of many runs with each mixture, using method (1) and method (2). Figure 4 also shows freezing-curve measurements using method (3) on mixtures of 59.6% and 82.3% He^3 in He^4 and on pure He^3. The experimental points are shown for these three concentrations. The curves for all of the mixtures reach lower pressures than those for either pure substance, indicating that solid mixtures can exist at lower pressure than the pure substances. The most striking feature of these results is that all mixtures have freezing curves which tend to merge into a common line below about 0.6°K with the exception of the 4.69% mixture. This behavior can be explained in terms of three-phase equilibrium.

The Gibbs phase rule relates the number of coexisting phases, ϕ, to the number of components c according to the equation

$$\phi + f = c + 2 ,$$

where f is the variance or the number of thermo-

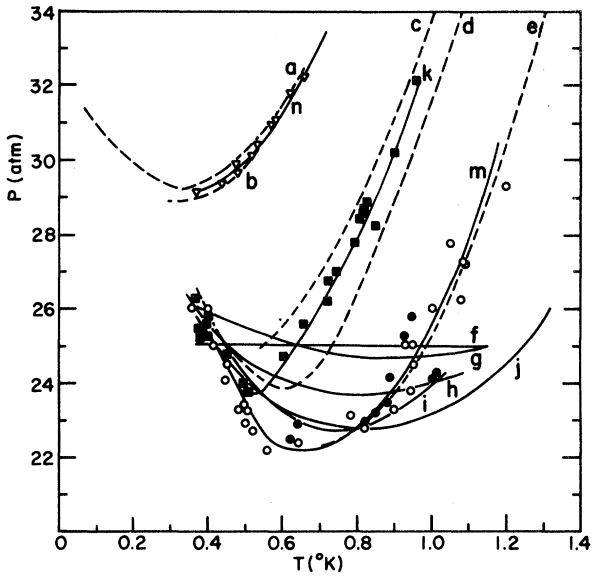

FIG. 4. The solid curves correspond to data obtained in this laboratory by strain-gauge techniques for various concentrations of He.[3] n (data points indicated by symbol ▽) – 100% (pure He^3), k (■) – 82.3%, m (○ – strain-gauge data, ● – NMR data) – 59.6%. Experimental points are not shown for the remaining curves because the strain gauges used in taking the data corresponding to them were temperature dependent and the necessary temperature corrections were made using the smoothed data. f – 0% (pure He^4), g – 4.69%, h – 18.8%, i – 38.4%, j – 24.2%. The dashed lines are results obtained at other laboratories by other techniques. a – 100%,[7] b – 100%,[23] c – 84.2%,[22] d – 80.1%,[11] e – 60.3%.[22]

dynamic degrees of freedom. In fact, f is the number of variables chosen from the pressure, temperature, and independent concentration variables in the various phases which can be arbitrarily changed without disturbing the equilibrium. In the case of the He^3-He^4 binary system, $c = 2$ and the set of thermodynamic variables consists of the pressure, the temperature, and the concentration of He^3 in each of the coexisting phases. In particular, when three phases coexist in a binary system there is only one thermodynamic degree of freedom possible. If one of the thermodynamic variables is specified in this situation, then all of the other variables will be determined. In particular if the temperature of a system of three coexisting phases is chosen, then the pressure and also the concentrations in the three phases will be fixed. If the temperature is taken to be the independent variable, each of the other thermodynamic variables will depend only on the temperature.

Thus for each temperature there is a unique pressure at which the three-phase equilibrium can exist. The locus of equilibrium conditions in the P-T plane for a given set of three phases is then a curve called a univariant (variance equals one). This univariant is the analog of, for instance, a liquid-vapor coexistence curve for a one-component system. The location of the univariant and the concentrations in the three phases are independent of the concentration of the initially homogeneous mixture.

The results of Fig. 4 show the existence of just such a univariant for He^3-He^4 mixtures below 0.6°K. Since phase separation is known to occur in liquid He^3-He^4 mixtures under pressure,[2] it is reasonable to assume that two of the three phases in equilibrium are liquid phases. Since the crystal structure of the solid mixtures is known to be body-centered cubic (bcc) in this region,[6] we can infer that the three phases which are in equililibrium are the bcc solid and the two liquids, L_1 (He^4 rich) and L_2(He^3 rich). This univariant will henceforth be designated bcc_1-L_1-L_2.

Some of the results obtained by other groups[7,11,22,23] carrying on similar investigations have been represented as dotted lines for comparison in Fig. 4. Additional comparisons with results of other investigators will be presented later in the article. The pure He^4 freezing curve is flat below about 1°K within our precision. However, more precise investigations have shown a shallow minimum at 0.8°K and a negative slope of 0.008 atm/°K.[8,9] Our He^3 freezing curve lies somewhat below that of Baum *et al.*[7] but somewhat above that of Grilly *et al.*[23] Reference to Fig. 4 shows that the He^3 freezing curve minimum should be very sensitive to small amounts of He^4 impurity which may explain the discrepancies among the various He^3 results.

Since the univariant line is analogous to the ordinary liquid-vapor equilibrium of a one-component system, it might be expected that a generalization of the Clausius-Clapeyron equation might hold. The condition for phase equilibrium in a multicomponent system is that the chemical potentials for a given component are equal for all the coexisting phases. Using this condition and the Gibbs-Duhem relationship,[24] the following equation can be derived for the slope of the univariant curve:

$$\begin{aligned} dP/dT = [&(n_3^{\mathrm{bcc}}\bar{S}_3^{\mathrm{bcc}} + n_4^{\mathrm{bcc}}\bar{S}_4^{\mathrm{bcc}}) \\ &- (n_3^{L_1}\bar{S}_3^{L_1} + n_4^{L_1}\bar{S}_4^{L_1}) \\ &- (n_3^{L_2}\bar{S}_3^{L_2} + n_4^{L_2}\bar{S}_4^{L_2})] \\ &\times [(n_3^{\mathrm{bcc}}\bar{V}_3^{\mathrm{bcc}} + n_4^{\mathrm{bcc}}\bar{V}_4^{\mathrm{bcc}}) \\ &- (n_3^{L_1}\bar{V}_3^{L_1} + n_4^{L_1}\bar{V}_4^{L_1}) \\ &- (n_3^{L_2}\bar{V}_3^{L_2} + n_4^{L_2}\bar{V}_4^{L_2})]^{-1} , \end{aligned}$$

where the n_i^j are the number of moles of each component i in the respective phases j and the $\bar{V}_i^j$ and $\bar{S}_i^j$ are the respective partial molar volumes and entropies. This equation can be written in a more familiar way as follows:

$$dP/dT = \Delta S / \Delta V ,$$

where ΔS is the entropy change when a specified amount of solid is melted and ΔV is the accompanying volume change as for a one-component system.

The region of negative slope can be qualitatively understood in terms of this equation. Because the solid is always the higher pressure phase, thermodynamic stability requires that the volume of the solid is always less than the liquid volume. Thus a negative slope would imply that the solid entropy is greater than the liquid entropy. As the temperature is reduced, a number of ordering effects occur in the liquid. There are the phase separation, the superfluid ordering in the He^4 rich phase, and the Fermi liquid ordering in the He^3 rich phase. The onset of phase separation in the solid occurs at considerably lower temperatures and on the basis of experimental work on pure solid He^3, magnetic ordering in the solid probably does not occur until millidegree temperatures are achieved.[25,26] The analogue of the Clausius-Clapeyron equation cannot be used to estimate the entropy change on solidification until measurements of ΔV have been performed.

B. Freezing-Curve Measurements Below 0.4°K

With the second apparatus it was possible, using magnetic cooling, to make strain-gauge measurements of the freezing curves of the solutions in the temperature range from 0.15 to 0.5°K. Data taken with this apparatus are shown in Fig. 5. A preliminary account of this work has been previously published.[13] The freezing curve for a concentrated mixture containing 78% He^3 shows a negative slope below 0.37°K, whereas curves for the dilute mixtures containing 1%, 5%, 7.8%, and 18% He^3, respectively, have positive slopes at the lowest temperatures. With the 38% mixture, either a positive or a negative slope at the lowest temperatures could be obtained depending on the sample pressure before cooling to form solid. For example, an initial pressure of 32 atm at 1.4°K yielded a negative slope below 0.37°K while a starting pressure of 28.5 atm yielded a positive slope in the same temperature range. All of the mixtures except the 1% mixture appeared to follow the same freezing curve with negative slope above 0.37°K, in agreement with the data presented in the previous section.

During a typical run, the region of positive slope was not seen until the cooling reached about 0.25°K. At 0.25°K, the pressure suddenly dropped and a brief warming occurred. The mixture would then follow the positive-sloped freezing curve shown in Fig. 5 to the lowest temperature. On warming, the mixture would follow the positive-sloped freezing curve shown in Fig. 5 all the way up to 0.37°K, where it joins the curve with negative slope which it would then follow as the temperature increased. At the point where the positive-sloped curve meets the negative-sloped curve, a brief cooling took place. The effect seen during the cooling part of the run is attributed to supercooling. The data shown were taken only on warm up to avoid this apparently spurious effect.

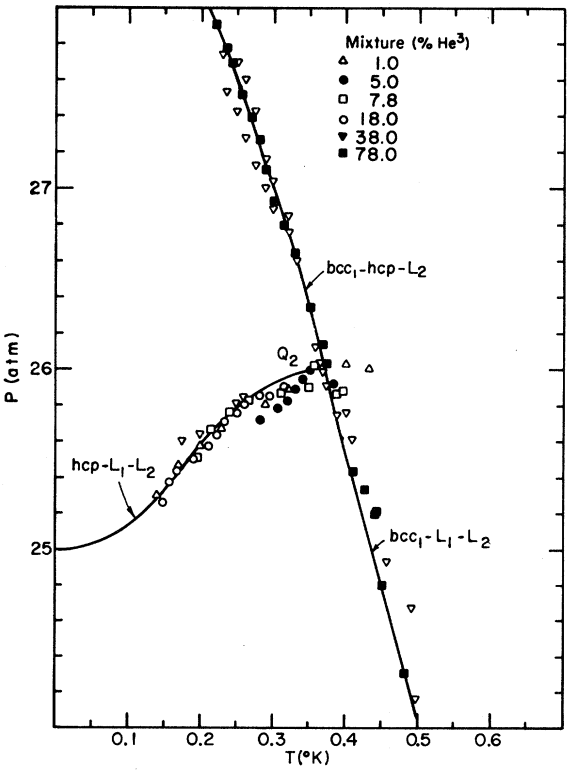

FIG. 5. Strain-gauge data for a number of mixtures obtained with the second apparatus. The locations of three-phase equilibrium lines are indicated.

The negative-sloped curve above 0.37°K has been interpreted to be the bcc_1-L_1-L_2 univariant as discussed in the previous section. The data in Fig. 5 show that the freezing curves of a wide range of mixtures also coincide for the region of positive slope below 0.37°K. This implies that the positive-sloped curve is also a univariant curve.

Below 0.37°K the liquid will consist of the two coexisting phases, the He^4-rich liquid L_1 and the He^3-rich liquid L_2. Since pure liquid He^4 and mixtures dilute in He^3 will solidify in the hexagonal close-packed (hcp) phase for high enough pressures and low enough temperatures,[6] it is reasonable to assume that L_1, if sufficiently dilute, will start to freeze into the hcp solid. Therefore we assume that the third coexisting phase is the hcp solid and is nearly pure He^4. The positive-sloped univariant is therefore labelled hcp-L_1-L_2.

The generalization of the Clausius-Clapeyron equation as applied to the hcp-L_1-L_2 univariant would imply that the entropy of the solid is less than the liquid entropy. This is reasonable if the solid is nearly pure He^4 and so has very little spin entropy and entropy of mixing. It is evident that there is still considerable entropy in the two liquids, since the He^4-rich phase still contains considerable[2] He^3, and the two liquids are not highly degenerate Fermi systems above 0.1°K.

It can be seen from Fig. 5 that above the pressure at which the hcp-L_1-L_2 and the bcc_1-L_1-L_2 univariants intersect, the negative-sloped curve continues on toward higher pressures and lower temperatures. Figure 5 also shows that mixtures with initial concentrations of 38% and 78% follow this curve, implying that this curve is a third univariant. At high enough pressures, it is reasonable to assume that the He^4-rich liquid L_1 will all be solidified. Hence the third univariant is assumed to involve three-phase equilibrium among the hcp solid, the bcc solid, and the He^3-rich liquid L_2, and is labeled bcc_1, -hcp-L_2. At the point of intersection of the three univariants, four phases coexist. This corresponds to a quadruple point which will be discussed in further detail in Sec. V.

As mentioned in Sec. II, exposure to magnetic fields during the adiabatic demagnetization procedure resulted in poor reproducibility in the Advance strain gauges at temperatures above 0.5°K making it difficult to obtain directly a proper absolute-pressure calibration. The absolute pressure was estimated by matching the portion of the negative-sloped curve, bcc_1-L_1-L_2, obtained with the first and second chambers in their common temperature range 0.37 to 0.50°K. An attempt was made to overcome this difficulty by using commercial strain gauges which were designed for use at low temperatures in magnetic fields. With these gauges it was possible to obtain an absolute pressure calibration to an accuracy of 0.3 atm by comparing strain-gauge readings with the pressure as determined from the external Bourdon gauge above 1°K.

C. Melting Curve of a 78% Mixture

The third experimental method (method 3) described in Sec. III was used to determine a portion of the melting curve and a portion of the freezing curve of a mixture with a 78% He^3 concentration. As the pressurized liquid sample was cooled, the sample chamber pressure indicated by strain-gauge measurements first began to drop at the onset of solidification corresponding to a point on the freezing curve. The sample chamber pressure continued to drop on further cooling until the chamber was filled with solid at which point the pressure became constant. This point corresponds to a point on the melting curve. Figure 6 shows points obtained on the freezing curve and the melting curve of the 78% mixture using this method with different starting pressures. Typical sets of data are shown in Fig. 7. The measured freezing curve is in good agreement with the freezing curve of a 78% mixture measured by Zinovieva[22] as shown in Fig. 6. At a given temperature, the freezing curve of this mixture is several atmospheres below the melting curve. The data obtained on these runs were reproducible on the warm up, indicating that the solid formed was probably fairly homogeneous, so that the melting curve point was really appropriate for the initial concentration. The time needed to cool down the sample until it became all solid was of the order of 8 to 10 h. In their phase-separation measurements, Edwards, McWilliams, and Daunt[5] noticed equilibrium times in the solid of less than a few minutes, indicating that the solid was probably homogeneous in these melting-curve experiments.

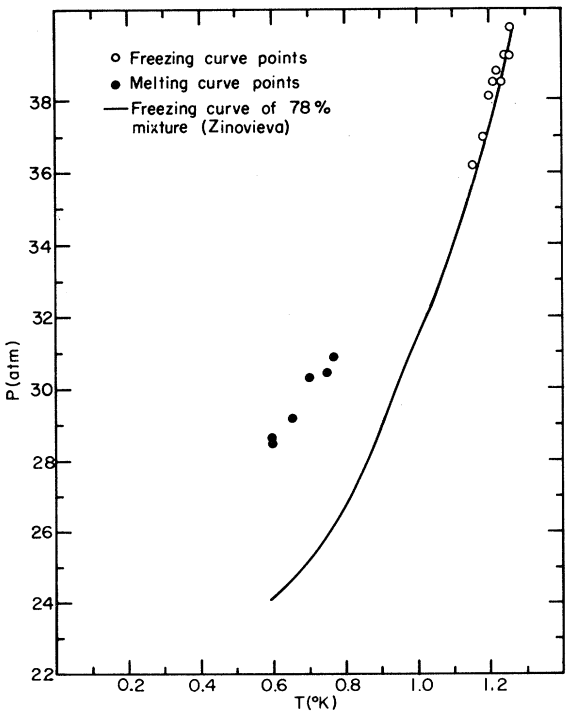

FIG. 6. Freezing and melting curves for the 78% mixture obtained with the second apparatus. The solid line is the freezing curve for a 78% mixture from Ref. 22.

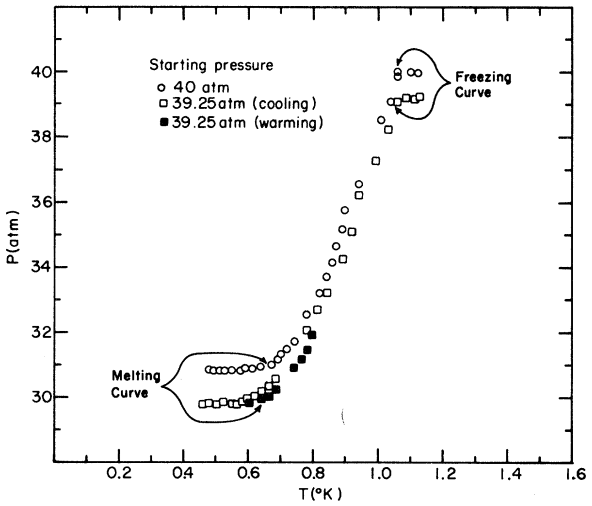

FIG. 7. Strain-gauge measurements on the 78% mixture showing how freezing and melting curve points were determined.

D. Phase Separation in Solid He^3-He^4 Mixtures

Edwards, McWilliams, and Daunt[5] discovered phase separation in solid He^3-He^4 mixtures by means of specific-heat measurements. The peak of the phase-separation curve was found by them to occur at 0.38°K. A similar experiment was carried out in this laboratory using the second apparatus described in Sec. II. The heat capacity of a mixture containing 78% He^3 was measured as

a function of temperature, and the results are shown in Fig. 8. The volume of the experimental chamber was 0.44 cm^3. Assuming the molar volume of the solid mixture to be 24 cm^3/mole, the value of C/R at the peak of the curve is 0.9 ± 0.1, whereas Edwards *et al.*[5] find a value of 1.0 for a 79% mixture. The temperature corresponding to the onset of phase separation is in good agreement with the results of Edwards *et al.*[5] The melting-curve measurements discussed above provide reasonable assurance that the specific-heat peak is in a region of the phase diagram where only solid is present.

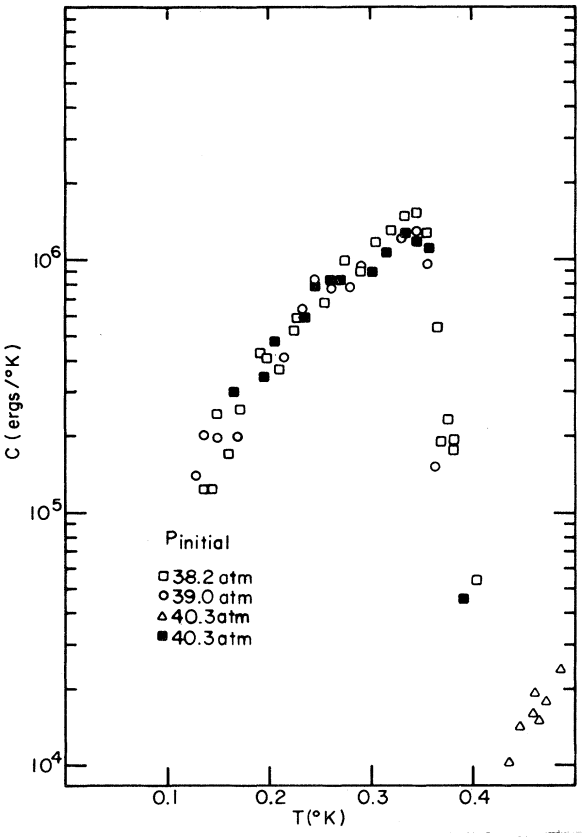

FIG. 8. Heat-capacity measurements on the 78% mixture for several initial pressures. The final pressure of the sample was about 9 atm lower than the initial pressure.

V. PROPOSED PHASE DIAGRAM

A phase diagram is proposed in an attempt to understand the complex behavior of He^3-He^4 mixtures observed in this work and in the work done at other laboratories. The following phenomena were taken into account in the construction of this phase diagram:

(i) phase separation in liquid He^3-He^4 mixtures,[1,2]

(ii) phase separation in solid He^3-He^4 mixtures,[5]

(iii) the hcp-bcc phase transition in solid He^3-He^4 mixtures,[6]

(iv) the behavior of the freezing curves of He^3-He^4 mixtures described in this work and also by others.[11,22]

A preliminary version of this phase diagram has been previously published.[12]

A useful way to begin discussion of the construction of the phase diagram is with a further examination of the Gibbs phase rule, which was introduced in Sec. IV(A). Since $\phi \geq 1$, the maximum value for f is three for a two-component system. Thus the representation of a binary system requires a three-dimensional phase diagram. In this case, the three variables are the pressure, P, the temperature, T, and the He^3 concentration, X. The maximum number of phases which can coexist is four, in which case $f = 0$. This condition defines a quadruple point and can only exist at isolated points in the PTX space. The quadruple point is the analog of a triple point in a single-component system.

The situation with three phases in equilibrium and $f = 1$ has been discussed in Sec. IV(A). The univariant or three-phase equilibrium is represented in PTX space by a ruled surface whose projection is a curve in the P-T plane as is shown schematically in Fig. 9 for the bcc_1-L_1-L_2 univariant. The location of two-phase and single-phase regions are also indicated in the figure.

The intersection of univariants is a quadruple point corresponding to the coexistence of four phases. A quadruple point will always be the intersection of four univariants[27] (three-phase equilibrium lines) since there are four ways of combining four phases taken three at a time. The analog for a single-phase system is the intersection of three two-phase equilibrium lines at a triple point. The intersection of the univariants bcc_1-L_1-L_2, hcp-L_1-L_2, and bcc_1-hcp-L_2 observed experimentally implies the existence of the qua-

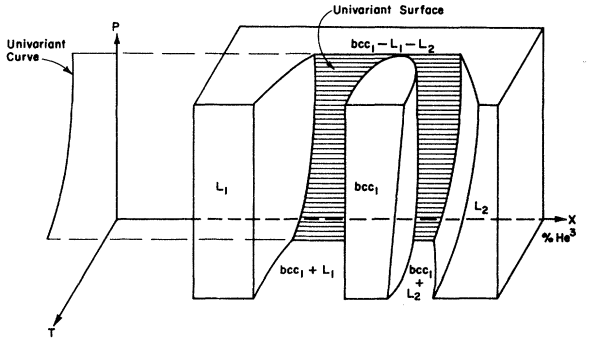

FIG. 9. Schematic PTX diagram of the univariant surface along which the bcc_1 solid and the two phase-separated liquids are in equilibrium.

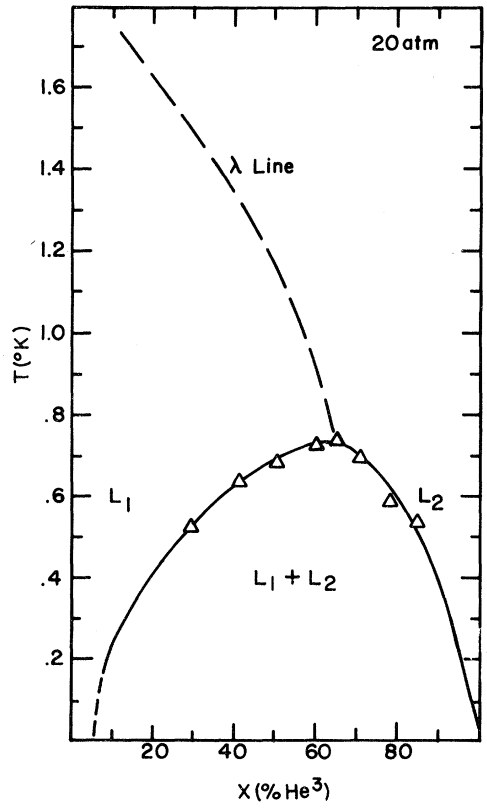

FIG. 10. The phase separation in liquid He^3-He^4 mixtures. Δ – Zinovieva.[22] It is not known if the phase separation is complete at 0°K and at elevated pressures. The λ line is extrapolated to meet the phase separation at its peak.

druple point bcc_1-L_1-L_2-hcp and a fourth intersecting univariant bcc_1-hcp-L_1.

A number of other rules[27] must also be kept in mind when constructing a phase diagram. In a *T-X* plane, if the liquidus and solidus corresponding to the onset of solidification and onset of melting, respectively, have a maximum or minimum, they must touch at the extremum point (Gibbs-Konovalow theorem).[28] This point of contact is an azeotropic point and the locus of azeotropic points in *PTX* space is an azeotropic line or line of equal concentration.

A critical line and a univariant line (three-phase line) both end at their intersection. At the intersection of a pure substance line, such as the melting curve of pure He^3 or pure He^4, with an azeotropic line, only the latter comes to an end, with the azeotropic line being tangent to the pure substance line. The same is true for the intersection of an azeotropic line with a univariant line.

Finally, the intersection of a pure substance line with a univariant must occur at the pure substance triple point corresponding to the equilibrium of those three phases which are in equilibrium along the univariant.

The phase diagram is presented as a series of *T-X* diagrams, each drawn for a different pressure. Only those curves where data points are shown have been experimentally verified. The experimental points shown in the figures have been taken from the results of this work and the results of other investigators.

At pressures lower than those needed for the formation of solid, the only feature of the phase diagram is the liquid phase separation which gives rise to the two liquids L_1 and L_2 as shown in Fig. 10. The lambda line is shown to intersect the phase separation at its peak in accordance with work done in this laboratory at saturated vapor pressure.[29] It has not been established whether phase separation is complete at the higher pressures, although it is known to be incomplete at saturated vapor pressure.[3,4] As the pressure is increased, the solid appears. Existing results are not accurate enough to establish with certainty whether the solid first nucleates outside or inside the liquid phase separation region. Figures 11 and 12 show sequences of *T-X* diagrams for each of these possibilities, respectively. The

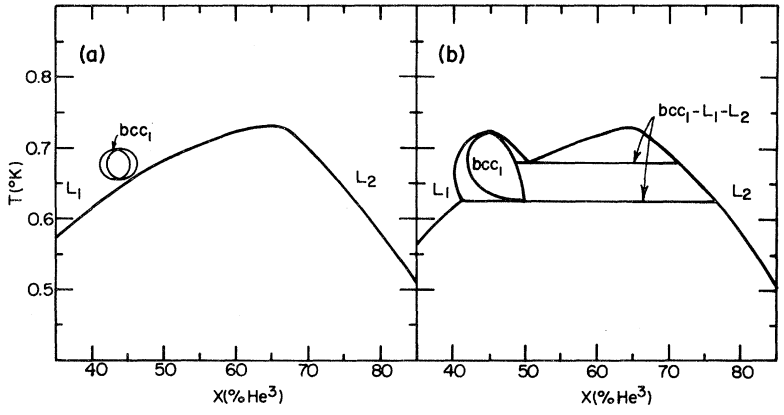

FIG. 11. (a) The bcc_1 solid has formed outside the liquid phase separation region. This case leads to a minimum in the azeotropic line. (b) At a slightly higher pressure the bcc_1 solid region has increased and intersected the liquid phase separation giving rise to univariant bcc_1-L_1-L_2.

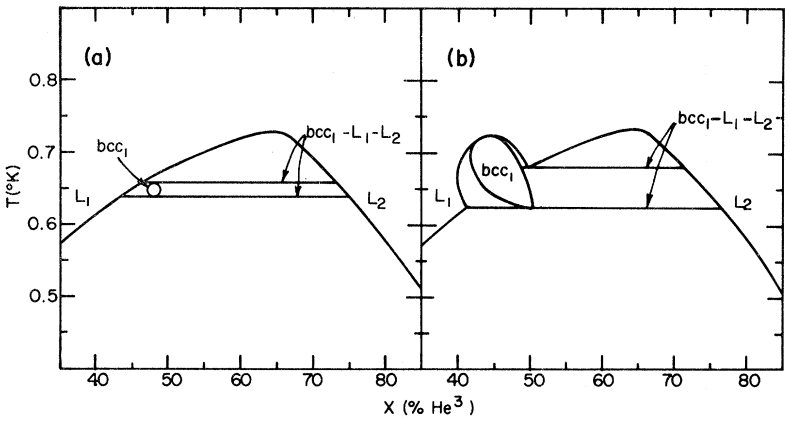

FIG. 12. (a) The bcc_1 solid has formed inside the liquid phase separation region giving rise to the univariant bcc_1-L_1-L_2. (b) At a slightly higher pressure, the bcc_1 solid region has increased and the situation is identical to that in Fig. 11(b).

first possibility leads to a minimum in the azeotropic line on the P-T diagram while the second does not. The pressure at which solid first forms and the concentration of this solid were chosen to be 22.8 atm and 45%, respectively, as inferred by LePair *et al.*[11]

Both sequences lead to Fig. 13. Here, at 24 atm, the solid, which has body-centered cubic (bcc) crystal structure, is a well-established island surrounded by liquid. This is related to the fact that He^3-He^4 mixtures can exist as a solid at pressures below the lowest melting pressure of either He^3 or He^4. The liquid phase separation is still evident at the bottom of the figure. The horizontal line labeled bcc_1-L_1-L_2 is the intersection of the T-X plane $P = 24$ atm with the ruled univariant surface along which bcc_1, L_1, and L_2 are in equilibrium. Choosing P determines both the temperature and the concentrations of the

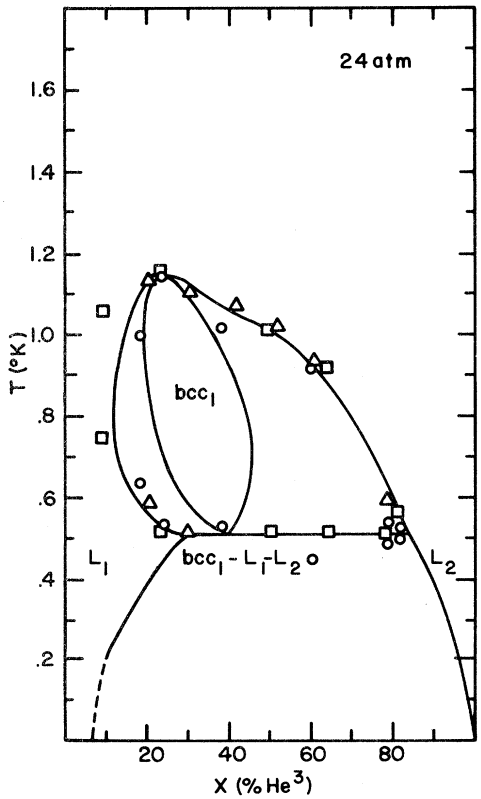

FIG. 13. At 24 atm the bcc_1 solid region has become larger and the peak of the liquid phase separation has disappeared. ○ This work; □ LePair *et al.*[11]; △ Zinovieva.[22]

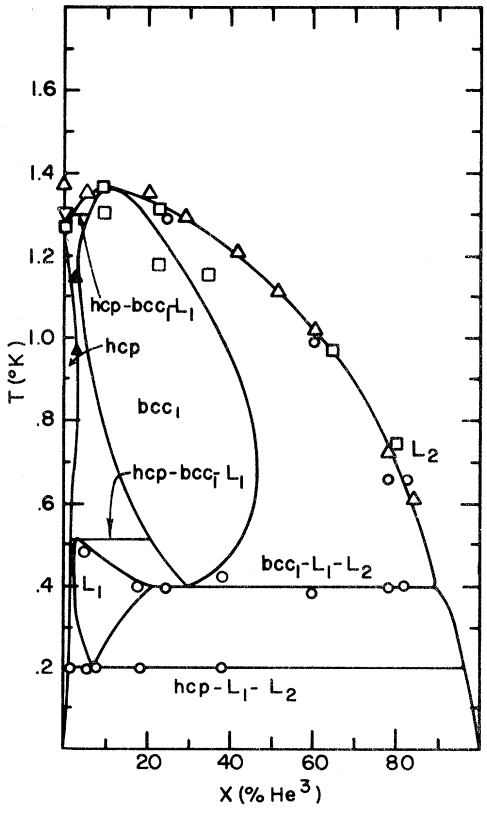

FIG. 14. At 25.6 atm the hcp solid has formed, isolating a region of liquid L_1. Three univariants are shown. ○ This work; ▽ Vignos and Fairbank[6]; □ Le Pair *et al.*[11]; △ Zinovieva[22]; ▲ Lipschultz *et al.*[30]

three phases in accordance with the discussion of the phase rule. Figure 13 resembles an ordinary eutectic diagram with two liquids and one solid rather than two solids and one liquid coexisting.

Figure 14 is drawn for a pressure of 25.6 atm. The question of what happens as the He^4-rich hexagonal close-packed (hcp) solid begins to form at about 25.0 atm is related to the melting curve minimum in pure He^4. This is treated in detail by LePair *et al.*[11] and will not be discussed here. At 25.6 atm, the hcp solid stretches along the left side of the diagram and has isolated a pocket of liquid, L_1. Two more univariants have appeared, hcp-L_1-L_2 and hcp-bcc_1-L_1. The univariant hcp-bcc_1-L_1 appears twice because it is thought to have a minimum in the P-T plane, and the plane $P = 25.6$ atm cuts it at two different temperatures. The projections of the hcp-L_1-L_2 and bcc_1-L_1-L_2 univariants in Fig. 14 onto the P-T plane are shown in Fig. 5. These figures show that hcp-bcc_1-L_1 and bcc_1-L_1-L_2 move to lower temperatures as P increases while hcp-L_1-L_2 moves to higher temperatures.

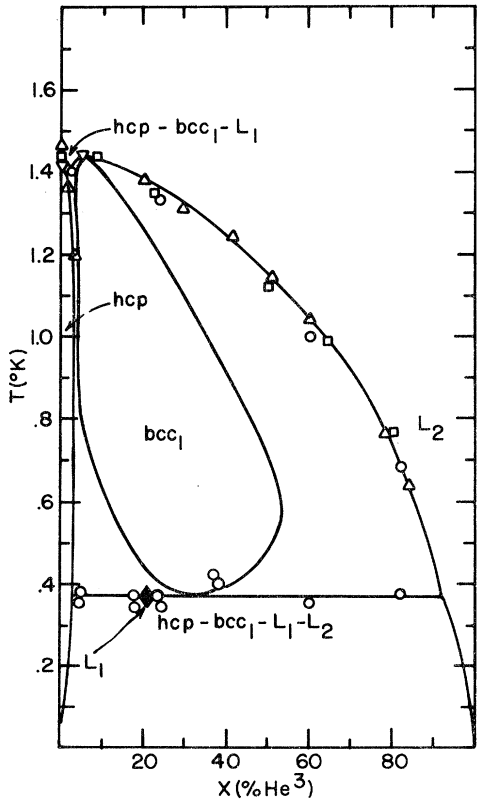

FIG. 15. At 26 atm and 0.37°K, the four phases, hcp solid, bcc_1 solid, liquid L_1, and liquid L_2 are in equilibrium, i.e., a quadruple point exists at this temperature and pressure. ○ This work; ▽ Vignos and Fairbank[6]; □ Le Pair *et al.*[11]; △ Zinovieva[22]; ▲ Lipschultz *et al.*[30]

In Fig. 15 at 26 atm the three univariants in Fig. 14 have met at about 0.37°K. At higher pressures, no He^4-rich liquid L_1 can exist. This point is the quadruple point labelled Q_2 deduced from the experimental results earlier in the paper [Sec. IV(B)] corresponding to the coexistence of four phases, hcp, bcc_1, L_1, and L_2. The four intersecting univariants associated with this quadruple point are bcc_1-L_1-L_2, hcp-L_1-L_2, bcc_1-hcp-L_1, and bcc_1-hcp-L_2.

The interpretation of the experimental results obtained in this work in terms of a quadruple point is supported by observations by Zinovieva[22] who visually detected the stratification of an 86.3% mixture into two liquid phases at temperatures of 0.30 and 0.35°K and a pressure of 26 atm with no what determine the path of bcc_1-hcp-L_2. Since pure liquid He^3 and pure solid He^3 are in equilibrium along the He^3 melting curve, the behavior shown in Fig. 20 is reasonable if the hcp solid is pure He^4 at absolute zero.

The hcp-L_1-L_2 curve is shown merging into the pure He^4 melting curve as the temperature approaches zero. If Fig. 14 is correct, then as the pressure decreases from 25.6 atm and the hcp-L_1-L_2 line moves toward lower temperatures, L_1 and L_2 become purer until at absolute zero the pure hcp solid will be in equilibrium with the pure He^4 and pure He^3 liquids assuming complete phase separation at absolute zero. In this condition the solid will be at the bottom of a container with the He^4 liquid above it and the He^3 liquid on top. If phase separation is complete at absolute zero, He^3 atoms cannot spontaneously pass into either liquid He^4 or solid He^4 whereas the He^4 atoms can move freely from liquid to solid. Thus it seems reasonable that the three-phase equilibrium curve hcp-L_1-L_2 should extrapolate to the He^4 melting curve. If the liquid phase separation is incomplete at absolute zero, as is the case for saturated vapor pressures[3,4] that is, if L_1 can have finite concentration of He^3 at absolute zero, then the situation can be quite different. If the hcp solid meets the liquid phase separation surface in such a way that it "traps" a region of L_1 on the low-temperature side, then the univariant hcp-L_1-L_2 will have a minimum. Figure 21 shows a series of T-X diagrams for incomplete phase separation which leads to a minimum in the hcp-L_1-L_2 line on the P-T diagram.

The other univariants end more routinely. Figures 11 and 12 show why bcc_1-L_1-L_2 must end at the peak of the liquid phase separation. The termination of bcc_1-bcc_2-L_2 at the critical point of the solid phase separation can be understood by noticing how Fig. 17 evolves from Fig. 16. Less is known about the termination of bcc_1-bcc_2-hcp. It is thought that the critical curve (labeled CP) for the solid phase separation is nearly independent of pressure.[5] As the pressure is in-

creased the hcp-bcc phase transition occurs at higher He^3 concentrations. As the hcp-bcc transition moves across toward higher He^3 concentrations, it carries bcc_1-bcc_2-hcp with it until it hits the peak of the curve, CP in Fig. 19. At this point on the P-T diagram bcc_1-bcc_2-hcp should terminate. Very little is known about the solid phase separation, however, so this statement lacks verification. Finally, the bcc_1-hcp-L_1 line must end at the pure He^4 melting curve at the lower triple point. In Fig. 20, points shown on the bcc_1-hcp-L_1 univariant were obtained by Lipschultz *et al.* in ultrasonic experiments.[30] From the shape of the T-X diagrams in Figs. 10–19, the location of the azeotropic line on the P-T diagram is also solid being present. These observations agree qualitatively with the data in Fig. 5 and with the proposed phase diagram presented here if her observations were made in the two-phase region between hcp-L_1-L_2 and bcc_1-L_1-L_2 (Fig. 14). In the same manner that a triple point is useful in establishing a fixed temperature point in a single-phase system, a quadruple point in the He^3-He^4 system provides a fixed temperature point below 1°K, which is not a function of pressure or impurity content.

The location of the line bcc_1-hcp-L_2 is shown in Fig. 16 at 26.2 atm. This line also appears in Fig. 5. In the high-temperature region of the diagram, the univariant hcp-bcc_1-L_1 has disappeared and the boundaries of the two solid phases have met at the X = 0 axis. This point corresponds to the lower triple point[6] in pure He^4.

In Fig. 17 at 26.5 atm, the solid-phase separation[5] first appears and is thought to be a phase separation into two bcc phases labeled bcc_1 and bcc_2. This gives rise to another univariant, bcc_1-bcc_2-L_2. CP marks the critical point of the solid-phase separation. Along the pure He^4 axis, the thin region of bcc solid[6] in pure He^4 is in evidence at about 1.5°K. The data points in this figure belong to the bcc_1-hcp-L_2 line and not to the bcc_1-bcc_2-L_2 univariant. The projection of the two univariants onto the PT plane is shown in Fig. 20.

At 26.75 atm, in Fig. 18, the univariants bcc_1-bcc_2-L_2 and bcc_1-hcp-L_2 have met, giving rise to a second quadruple point, with the four phases bcc_1, bcc_2, hcp, and L_2 coexisting.

Again there must be four univariants meeting at this quadruple point. The other two, bcc_1-bcc_2-hcp and bcc_2-hcp-L_2, are shown in Fig. 19 at 30 atm. These surfaces, too, are shown in Fig. 20, projected onto the P-T plane. At 30 atm, pure He^3 has begun to solidify, isolating a small pocket of L_2 in the lower right-hand corner. This is related to the minimum in the He^3 freezing curve.

The location of all of the univariant surfaces is summarized in Fig. 20 where their projections on the P-T plane are shown. The parts of the surfaces which have been measured in this laboratory have data points shown.

A few words must be said concerning the extrapolation of some of the univariants beyond the region where they have been measured. The ways of terminating univariants were mentioned earlier in this section. They can terminate at critical point lines or pure substance lines, and at quadruple points where four must meet.

The bcc_1-hcp-L_2 univariant has been drawn so that it meets the pure He^3 melting curve at high pressure and low temperature. This must be the case if the hcp solid is essentially inert and does not affect the situation at all. Then nearly pure solid He^3 (bcc_1) and nearly pure liquid He^3 (L_2) are clear.

Large portions of the phase diagram and the existence of many of the three-phase surfaces have not been verified experimentally suggesting the need for further experiments.

Alternative diagrams have been suggested by several other groups.[11,22,31] The diagram proposed by LePair *et al.*[11] mainly agrees with the one presented here. In addition, they discuss the

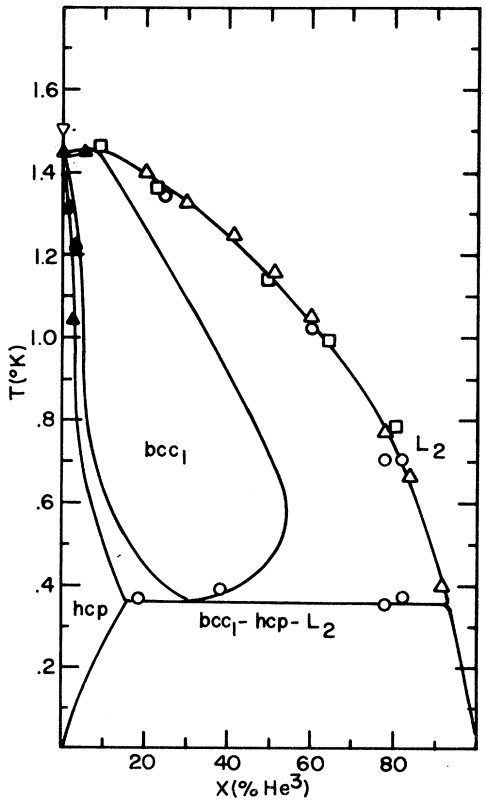

FIG. 16. At 26.2 atm only the univariant bcc_1-hcp-L_2 remains. L_1 cannot exist at this pressure. The lower triple point of pure He^4 is at about 1.45°K.[6] ○ This work; ▽ Vignos and Fairbank[6]; □ Le pair *et al.*[11]; △ Zinovieva[22]; ▲ Lipschultz *et al.*[30]

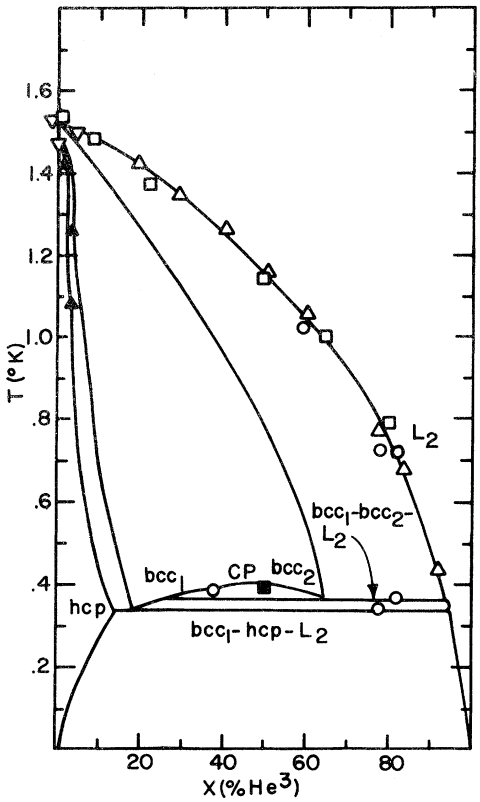

FIG. 17. At 26.5 atm the solid phase separation has appeared giving rise to a second bcc solid bcc_2 and a new univariant bcc_1-bcc_2-L_2. ○ This work; ▽ Vignos and Fairbank[6]; □ Le Pair *et al.*[11]; △ Zinovieva[22]; ▲ Lipschultz *et al.*[30]; ■ Edwards *et al.*[15]

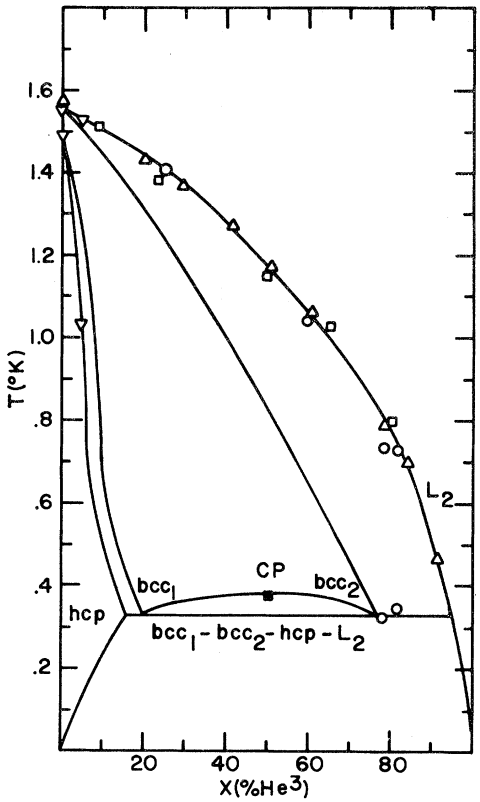

FIG. 18. At 26.75 atm and 0.33°K a second quadruple point occurs corresponding to the equilibrium of bcc_1 and bcc_2 solids, hcp solid and liquid L_2. ○ This work; ▽ Vignos and Fairbank[6]; □ Le Pair *et al.*[11]; △ Zinovieva[22]; ■ Edwards *et al.*[15]

phenomena related to the minimum of the He^4 freezing curve and the formation of the hcp solid. They also propose an alternative for the behavior of the crystallographic phase transition, and consequently, for the existence of the upper quadruple point. This alternative requires that as the pressure increases, the two-phase region between the hcp and bcc solids increases at the low temperature end and that the solid phase separation starts to grow on the low He^3 concentration side of the bcc solid. As soon as this happens, the univariant bcc_1-bcc_2-hcp appears. Figure 22 illustrates this possibility along with the relevant P-T diagram. As LePair *et al.*[11] point out, there are no data available to allow a choice to be made between these two possibilities.

VI. CONCLUSION

Over the range of temperatures and pressures so far investigated, the proposed phase diagram agrees well with experiment. The experiments performed in this laboratory have demonstrated the existence of a quadruple point for He^3-He^4 mixtures and the existence of several univariant lines in the liquid-solid phase transition including some which have a negative slope on the P-T diagram. Extensions of these measurements to lower temperatures and higher pressures would be of interest. To understand the thermodynamics of the univariant lines, measurements of the volume change that occurs when liquid is converted to solid would also be useful.

ACKNOWLEDGMENTS

We wish to thank Dr. C. F. Kellers, Dr. F. P. Lipschultz, and Dr. H. Weinstock for helping with the design and construction of the apparatus. We are also grateful to Professor Watt W. Webb and Professor Benjamin Widom for a number of useful and stimulating discussions regarding the construtions of phase diagrams.

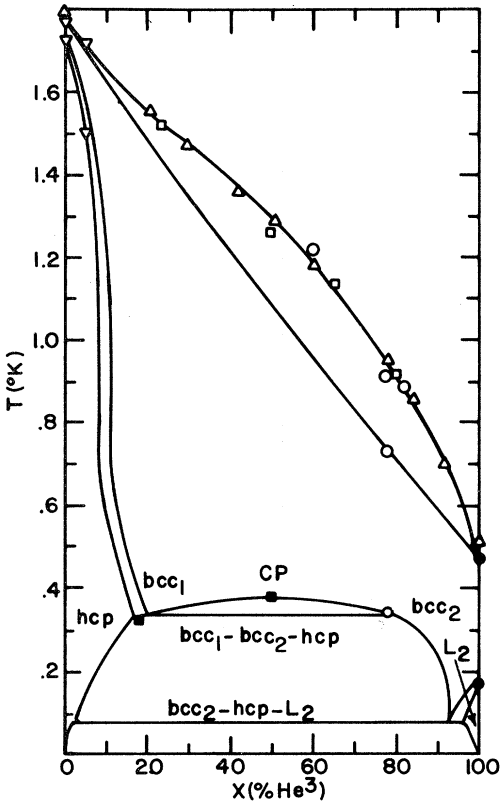

FIG. 19. At 30 atm pure He^3 has started to solidify. The figure shows two univariants bcc_1-bcc_2-hcp and bcc_2-hcp-L_2. ○ This work; ▽ Vignos and Fairbank[6]; □ Le Pair *et al.*[11]; △ Zinovieva[22]; ■ Edwards *et al.*[15]; ● Baum *et al.*[7]

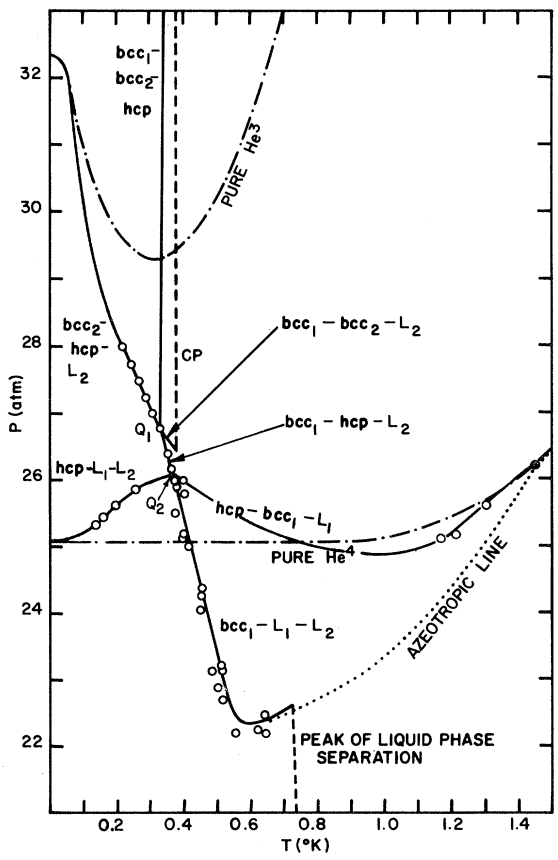

FIG. 20. The projections of the univariant surfaces shown in the T-X diagrams (Figs. 11 through 19) are projected onto the P-T plane. Also shown are the freezing curves of pure He^3 and pure He^4, the azeotropic line, the critical point line CP of the solid phase separation and the locus of the peaks of the liquid phase separation. The quadruple points are labeled Q_1 and Q_2. Only the portions of the univariants with data points have been verified in this laboratory. The methods used in extrapolating these curves are discussed in the text.

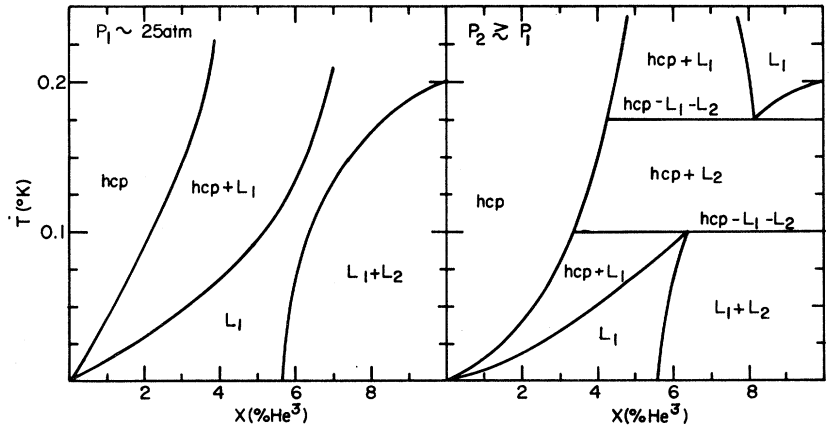

FIG. 21. T-X diagrams showing the possibility of a minimum in the univariant hcp-L_1-L_2 if liquid phase separation is not complete at $T = 0°$ K.

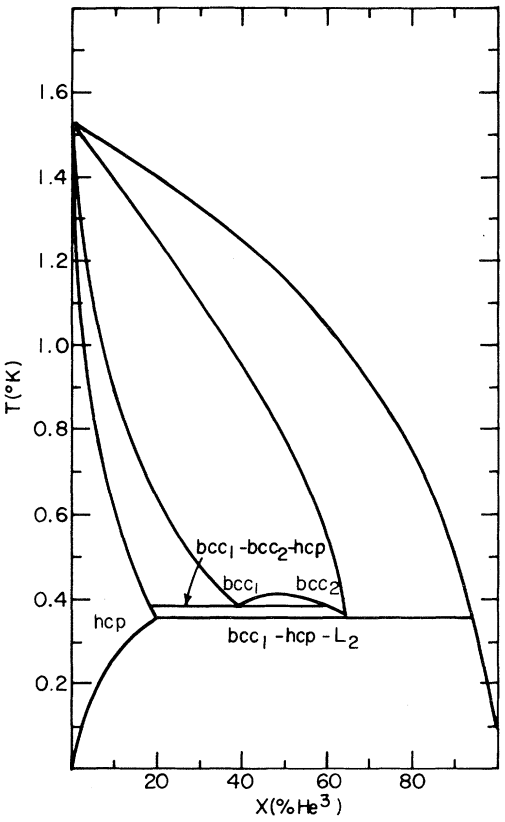

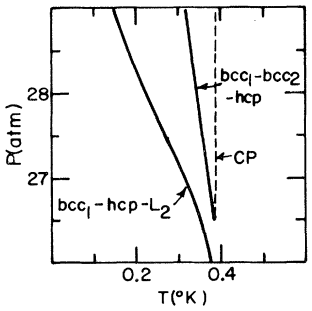

FIG. 22. Alternative possibility of the emergence of the solid phase separation[11] which does not require the quadruple point Q_1.

*Work supported by the National Science Foundation (GP-8148) and the Advanced Research Projects Agency through the Materials Science Center at Cornell University, Report No. 978.

†Present address: Francis Bitter National Magnet Laboratory, Massachusetts Institute of Technology, Cambridge, Massachusetts.

‡This paper is based on a thesis submitted by P. M. Tedrow to Cornell University in partial fulfillment of the requirements for the Ph. D. degree.

[1]G. K. Walters and W. M. Fairbank, Phys. Rev. 103, 262 (1956).

[2]K. N. Zinovieva and V. P. Peshkov, Zh. Eksperim. i Teor. Fiz. 37, 33 (1959) [English transl.: Soviet Phys. – JETP 10, 22 (1960)].

[3]D. O. Edwards, D. F. Brewer, P. Seligman, M. Skertic, and M. Yaqub, Phys. Rev. Letters 15, 773 (1965).

[4]O. E. Vilches and J. C. Wheatley, Phys. Letters 24A, 440 (1967); 25A, 344 (1967).

[5]D. O. Edwards, A. S. McWilliams, and J. G. Daunt, Phys. Rev. Letters 9, 195 (1962).

[6]J. H. Vignos and H. A. Fairbank, Phys. Rev. 147, 185 (1966).

[7]J. L. Baum, D. F. Brewer, J. G. Daunt, and D. O. Edwards, Phys. Rev. Letters 3, 127 (1959).

[8]C. Le Pair, K. W. Taconis, R. De Bruyn Oubuter, and P. Das, Physica 29, 755 (1963).

[9]G. C. Straty and E. D. Adams, Phys. Rev. Letters 17, 290 (1966).

[10]H. Weinstock, F. P. Lipschultz, C. F. Kellers, P. M. Tedrow, and D. M. Lee, Phys. Rev. Letters 9, 193 (1962).

[11]C. Le Pair, K. W. Taconis, R. De Bruyn Oubuter, P. Das, and D. de Jong, Physica 31, 764 (1965).

[12]P. M. Tedrow and D. M. Lee, Phys. Letters 9, 130 (1964).

[13]P. M. Tedrow and D. M. Lee, Phys. Rev. Letters 13, 388 (1964).

[14]Baldwin-Lima-Hamilton Corporation, Electronics and Instrumentation Division, Waltham, Massachusetts.

[15]C. Blake, C. E. Chase, and E. Maxwell, Rev. Sci. Instr. 29, 715 (1958).

[16]Speer Carbon Company, Bradford, Pennsylvania.

[17]H. Weinstock, F. P. Lipschultz, C. F. Kellers, and D. M. Lee, Proceedings of Eighth International Conference on Low Temperature Physics, edited by R. O. Davies (Butterworth Scientific Publications, Ltd., London, 1963), p. 41.

[18]Advance is a 43% Nickel 57% Copper alloy manufactured by the Driver-Harris Company, Harrison, New Jersey.

[19]Duco Household Cement, E. I. du Pont de Nemours and Co., Inc., Wilmington, Delaware.
[20]Castolite Co., Woodstock, Illinois.
[21]0–50-atm gauge, calibrated in 0.05-atm steps. Heise-Bourdon Tube Company, Newtown, Connecticut.
[22]K. N. Zinovieva, Zh. Eksperim. i Teor. Fiz. 44, 1837 (1963) [English transl.: Soviet Phys. – JETP 17, 1235 (1963)].
[23]R. L. Mills, E. R. Grilly, and S. G. Sydoriak, Ann. Phys. 12, 41 (1961).
[24]I. Prigogine and R. Defay, Chemical Thermodynamics (Longman's Green and Co., Inc., New York, 1954) p. 71.
[25]R. C. Richardson, E. Hunt, and H. Meyer, Phys. Rev. 138, A1326 (1965).
[26]M. F. Panczyk, R. A. Scribner, G. C. Straty, and E. D. Adams, Phys. Rev. Letters 19, 1102 (1967).
[27]L. D. Landau and E. M. Lifshitz, Statistical Physics (Pergamon Press, Ltd., New York, 1960) p. 310.
[28]See Ref. 24, p. 281.
[29]E. H. Graf, D. M. Lee, and J. D. Reppy, Phys. Rev. Letters 19, 417 (1967).
[30]F. P. Lipschultz, P. M. Tedrow, and D. M. Lee, in Proceedings of the Ninth International Conference on Low Temperature Physics, Columbus, 1964, edited by J. G. Daunt *et al.* (Plenum Press, Inc., New York, 1965), p. 254.
[31]N. G. Berezniak, I. V. Bogoyavlensky, and B. N. Eselson, Zh. Eksperim. i Teor. Fiz. 45, 486 (1963), [English transl.: Soviet Phys. – JETP 18, 335 (1964)].

PHYSICAL REVIEW VOLUME 181, NUMBER 1 5 MAY 1969

Heat of Mixing and Ground-State Energy of Liquid He^3-He^4 Mixtures*

P. Seligmann, D. O. Edwards, R. E. Sarwinski, and J. T. Tough
Department of Physics, Ohio State University, Columbus, Ohio 43210
(Received 24 January 1969)

The heat evolved when He^3 is added to liquid He^3-He^4 mixtures at the saturated vapor pressure has been measured for temperatures in the region of 0.05°K. The starting concentrations varied between zero and six atomic percent of He^3. Since the variation of the energy with temperature (the specific heat) is known, the experiments give the ground-state energy and the He^3 and He^4 chemical potentials at 0°K as a function of concentration. The measurements were made in a calorimeter connected by a wire of high thermal resistance to a dilution refrigerator operating at ~0.02°K. The He^3 was added through a long tube containing thermal anchors connected to the refrigerator.

The results give the difference in binding energy for one He^3 atom in He^4 relative to pure He^3 as $(E_3 - L_3{}^0)/k_B = (0.312 \pm 0.007)$ deg K, in excellent agreement with the theoretical value of Massey and Woo. The concentration dependence of the energy and chemical potentials agrees with predictions using the Bardeen, Baym, and Pines empirical interaction. The osmotic pressure in a saturated solution at 0°K is found to be (17.8 ± 0.9) mm Hg.

INTRODUCTION

In the experiment described here, we have measured as directly as possible the ground-state or 0°K energy of He^3-He^4 solutions as a function of X, the atomic concentration of He^3. The measurements have been carried out at zero pressure up to the limit of solubility of He^3 in He^4 which, according to the results of Ifft *et al.*,[1] is $X_0 = 6.4\%$. The present experiment was primarily undertaken to determine the binding energy of one He^3 atom in liquid He^4 (E_3 in our notation) to compare with recent theoretical estimates.[2–5] In addition, the variation of the ground-state energy with concentration and the derived chemical potentials at 0°K, $\mu_{30}(X)$ and $\mu_{40}(X)$, provide an excellent test of the empirical quasiparticle effective interaction constructed by Bardeen, Baym, and Pines (BBP).[3,6]

Theory of the Experiment

The energy of a mole of mixture at 0°K, $H_0(X)$, is conveniently described by the excess energy (or enthalpy, since $p = 0$), $H_0{}^E$, defined so that

$$H_0(X) = XH_0(X=1) + (1-X)H_0(X=0) + H_0{}^E(X)$$
$$= -XN_A L_3{}^0 - (1-X)N_A L_4{}^0 + H_0{}^E(X). \quad (1)$$